Optimization Issues in Combined Chip and Symbol Level Equalization for Downlink WCDMA Receivers

Ahmet Başтuğ* and Dirk T.M. Slock†
*Philips Semiconductors, 06560, Sophia Antipolis, FRANCE
tel: +33 4 9294 4130, fax: +33 4 9296 1280, e-mail: ahmet.bastug@philips.com
†Eurecom Institute, 06904, Sophia Antipolis, FRANCE
tel: +33 4 9300 2606, fax: +33 4 9300 2627, e-mail: slock@eurecom.fr

***Abstract*— Receiver structures that have been proposed for the WCDMA downlink comprise chip level channel equalizers to restore code orthogonality and symbol level Linear Minimum Mean Square Error (LMMSE) receivers that furthermore exploit subspace structure in the signal due to unused codes. In this paper we focus on receivers for high-speed downlink communications. The combined transmission system, comprising spreading and channel filtering, is time-varying at chip rate in WCDMA systems, which makes LMMSE receivers necessarily highly time-varying. We consider the case of multi-code high-rate communications (HSDPA) where inter-chip and inter-code interference dominate. We discuss optimization issues appearing in the advantageous combination of chip-level and iterative symbol-level equalization. Furthermore, iterative symbol-level operations allow for a continuous operation between linear and non-linear receivers.**

I. Introduction

In the UMTS downlink, high data rate can be provided to a user by either going to very small spreading factors (SFs), a more probable scenario for the Time Division Duplexed (TDD) mode, or by allocating multiple codes, e.g HSDPA in the Frequency Division Duplexed (FDD) mode. The techniques in order to combat the distortion effect of the multipath propagation channel are different for the two cases.

In the low spreading case, system performance might degrade significantly by the inter symbol interference (ISI) effect. On the one hand, this effect exists only for systems with periodic codes (e.g TDD mode). On the other hand, it is this periodicity which is exploited to apply symbol level equalization to mitigate the ISI after Rake reception, see [1] for the Rake-MLSE and [2] for the Rake-DFSE methods. These two techniques, however, do not much suppress interchip interference [3].

In the medium and high spreading cases ($SF \geq 16$, e.g FDD), ISI is negligible. In this case, multiaccess interference (MAI) and interchip interference (ICI) dominate. One state-of-the art method that copes with these effects is the parallel interference canceller (PIC) receiver which asymptotically converges to the *decorrelator receiver* [4]. However it requires very relaxed cell loads to converge. Even if it converges, the speed of convergence is very slow since estimated different user symbols are highly correlated [5], which in fact is a consequence of the low *orthogonality factors* that can be obtained initially from *the usage of Rake receivers* in the front-end [6], [7].

In this paper we elaborate on efficient methods corresponding to the medium and high spreading cases. We will cover the methods for the low spreading case in a forthcoming paper.

One particular application of interest is the high speed packet data access (HSDPA) service standardized in Release-5 of UMTS FDD standard [8], [9]. In HSDPA, one or more of the High Speed Downlink Shared Channels (HSDSCHs) at SF-16, in particular 1,5,10 or 15 of the 16 available codes, are time multiplexed (scheduled) among users, preferably all allocated to a single user at any time. The goal is to exploit *multiuser diversity*, i.e the temporal channel quality variance among the users, in order to increase the *sum capacity*, that is the total delivered payload by the BS. It is up to the operators to choose the types of schedulers that compromise throughput and fairness by taking the predicted channel quality, the cell load and the traffic priority class into account. A better performing mobile receiver is quite beneficial in HSDPA services since unlike for dedicated channels (DCHs) where it serves only for the benefit of the base station, for HSDSCHs, a mobile terminal directly benefits from having an advanced receiver by obtaining more data rate once the connection is established and by increasing the chance of getting a connection if fairness is partially sacrificed for capacity in user scheduling. Advanced interference canceller (IC) receivers might benefit from knowing possibly more than one equally-powered HSDSCH codes and some common channels such as the common pilot channel (CPICH) [10].

II. Multicode Pseudo-transmission

Interference cancellation has been rarely considered for the downlink since it requires the knowledge of where the active codes reside in the OVSF tree and what their powers are. However, it is possible to equivalently represent an active multi-rate transmission as a multi-code pseudo-transmission at any single SF-level L in the OVSF hierarchy. One simplified example (representing actually the TDD case) that contains

SFs ranging from 1 to 16 is given in Fig. 1. In this example, the nodes corresponding to active codes at SF-levels 4 and 8 are demonstrated by black bulbs. Their pseudo-equivalents at SF-level 16 (i.e $L = 16$) are demonstrated by zig-zag pattern bulbs.

One can detect the existence or absence of pseudo-codes at the pseudo-level by comparing the powers at their correlator outputs with a noise-floor threshold [11]. These multiple correlations can be implemented with $O(L\,logL)$ complexity by using Fast Walsh Hadamard Transformation (FWHT). Unitary FWHTs (U-FWHT) with proper dimensions can be logically/physically exploited to see/implement the two-way transformations between actual symbol sequences corresponding to the known codes (e.g HSDPA multicodes) at various SF-levels and their pseudo-symbol sequence equivalents at a single SF-level. Fig. 2 demonstrates the two-way transformations between L_2/L_1 consecutive (time-multiplexed) a_i actual symbols at level L_1 and L_2/L_1 parallel (code-multiplexed) $\tilde{a}_i$ pseudo-symbols at a larger SF-level L_2. $P_{\{L_2/L_1\}}/S$ and $S/P_{\{L_2/L_1\}}$ are parallel to serial and serial to parallel converters from/to a bus size L_2/L_1. When actual symbols reside at a higher SF-level, the two transformations have reverse roles.

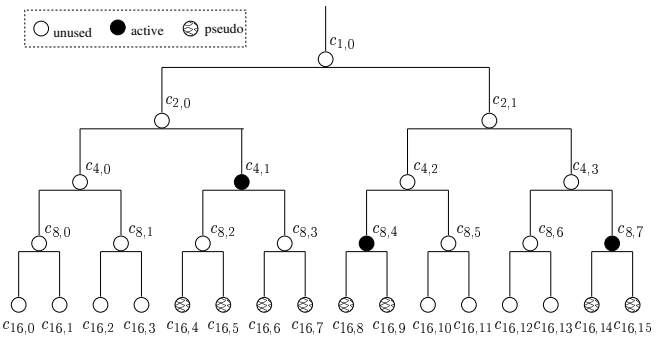

Fig. 1. Equivalency of active-multirate and pseudo-multicode systems

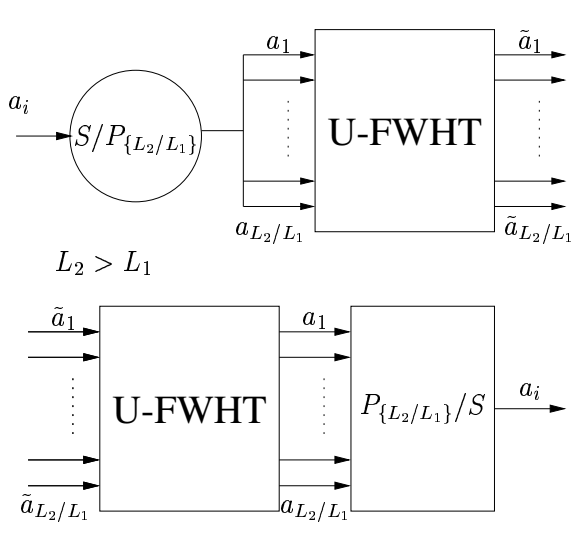

Fig. 2. Transformations between actual and pseudo symbols

III. Receiver Model

In this section, we develop parallel intra and intercell IC structures based on polynomial expansion (PE) technique which was initially proposed in [12]. We exploit the *pseudo-equivalency* concept at the highest *active* SF-level, SF-256, in the UMTS-FDD downlink for applying PE at this level. We ignore the existence of SF-512 since it is rarely used carrying control commands during an upload operation. The rationale for choosing the *highest active SF*, from now on called L, is to obtain the highest possible degree of freedom in determining the PE subspace. If any other level L_x were selected, then an activity on a child code of $c_{x,i}$, $i \in \{0,\ldots,L_x-1\}$, say at a level $L_y > L_x$ on $c_{y,j}$, $j \in \{(L_y/L_x)i,\ldots,(L_y/L_x)(i+1)-1\}$, would obligate the implicit inclusion of also all the other child codes of $c_{x,i}$ at level L_y by including $c_{x,i}$ in the PE. This would have an adverse effect of noise amplification.

Pseudo-codes might be used in place of the *unknown actual codes* since the actual symbol estimates and their powers are not necessary as long as the pseudo-symbols are treated linearly in interference cancellation. However, knowing or detecting the actual codes is an opportunity for exploiting hard or hyperbolic-tangent nonlinearities (or even channel decoding and encoding) to refine their symbol estimates [4], [13].

In a previous paper, we modeled the PE-based multistage receivers and elaborated mostly on single iteration architectures; see that paper for complete system definitions [14]. Here, we re-explain the derivations more concisely and then focus on multi-iterations.

Assuming without loss of generality that there is a single highly interfering BS, i.e. BS_2, a vector of received signal over one symbol period can be written as

$$\begin{aligned}\boldsymbol{Y}[n] &= [\boldsymbol{H}_1(z)\boldsymbol{S}_1[n]\boldsymbol{C}_1 \;\; \boldsymbol{H}_2(z)\boldsymbol{S}_2[n]\boldsymbol{C}_2] \begin{bmatrix}\boldsymbol{A}_1[n]\\ \boldsymbol{A}_2[n]\end{bmatrix} + \boldsymbol{V}[n] \\ &= \widetilde{\boldsymbol{G}}(n,z)\;\boldsymbol{A}[n] \;+ \boldsymbol{V}[n] \end{aligned} \quad (1)$$

$\boldsymbol{H}_j(z) = \sum_{i=0}^{M_j-1} \boldsymbol{H}_j[i]\, z^{-i}$ is the symbol rate $Lmq \times L$ channel transfer function, $\{z^{-1};\, m;\, q;\, M_j\}$ being {symbol period delay operator; oversampling factor w.r.t chip rate; number of antennas at the receiver side; channel spread in symbols}. The $L \times L$ matrices $\boldsymbol{S}_j[n]$ are diagonal and contain the scrambler of BS_j for symbol period n. The column vectors $\boldsymbol{A}_j[n]$ contain the K_j (pseudo-)symbols of BS_j, $\boldsymbol{A}[n]$ contain the total $K = K_1 + K_2$ (pseudo-)user (pseudo-)symbols in two base stations, and $\boldsymbol{C}_j$ is the $L \times K_j$ matrix of the K_j active codes for BS_j. $\widetilde{\boldsymbol{G}}(n,z)$ is the $Lmq \times K$ symbol rate channel-plus-spreading filter. $\boldsymbol{V}[n]$ is the $Lmq \times 1$ noise term which contains additive white Gaussian noise (AWGN) plus the unmodeled intercell interference.

We first consider a dimensionality reduction step (from Lmq to K) by equalizing the channels with minimum mean square error zero forcing (MMSE-ZF) chip rate equalizers $\boldsymbol{F}_j(z)$ followed by a bank of correlators [15].

Let $\boldsymbol{X}[n]$ be the $K \times 1$ correlator output, which would correspond to the Rake receiver outputs if channel matched

filters were used instead of channel equalizers. Then,

$$\begin{aligned}\boldsymbol{X}[n] &= \widetilde{\boldsymbol{F}}(n,z)\boldsymbol{Y}[n] \\ &= \begin{bmatrix} \boldsymbol{C}_1^H \boldsymbol{S}_1^H[n]\boldsymbol{F}_1(z) \\ \boldsymbol{C}_2^H \boldsymbol{S}_2^H[n]\boldsymbol{F}_2(z) \end{bmatrix} (\widetilde{\boldsymbol{G}}(n,z)\boldsymbol{A}[n] + \boldsymbol{V}[n]) \\ &= \boldsymbol{M}(n,z)\boldsymbol{A}[n] + \widetilde{\boldsymbol{F}}(n,z)\boldsymbol{V}[n]\end{aligned}$$

where $\boldsymbol{M}(n,z) = \widetilde{\boldsymbol{F}}(n,z)\widetilde{\boldsymbol{G}}(n,z)$ and ZF equalization results in $\boldsymbol{F}_j(z)\boldsymbol{H}_j(z) = \boldsymbol{I}$. Hence,

$$\boldsymbol{M}(n,z) = \sum_{i=-\infty}^{\infty} \boldsymbol{M}[n,i]z^{-i} = \begin{bmatrix} I & * \\ * & I \end{bmatrix}$$

due to proper normalization of the code energies.

In order to obtain the estimate of $\boldsymbol{A}[n]$, we initially consider the processing of $\boldsymbol{X}[n]$ by a decorrelator as

$$\begin{aligned}\widehat{\boldsymbol{A}}[n] &= \boldsymbol{M}(n,z)^{-1}\boldsymbol{X}[n] \\ &= (\boldsymbol{I} + \overline{\boldsymbol{M}}(n,z))^{-1}\boldsymbol{X}[n]. \end{aligned} \quad (2)$$

The correlation matrix $\boldsymbol{M}(n,z)$ has a coefficient $\boldsymbol{M}[n,0]$ with a dominant unit diagonal in the sense that all other elements of the $\boldsymbol{M}[n,i]$ are much smaller than one in magnitude. Hence, the polynomial expansion approach suggests to develop $(\boldsymbol{I} + \overline{\boldsymbol{M}}(n,z))^{-1} = \sum_{i=0}^{\infty}(-\overline{\boldsymbol{M}}(n,z))^i$ up to some finite order, which after dropping indices leads to

$$\begin{aligned}&\widehat{\boldsymbol{A}}^{(-1)} = 0 \;\; ; \;\; i \geq 0\,. \\ &\widehat{\boldsymbol{A}}^{(i)} = \boldsymbol{X} - \overline{\boldsymbol{M}}\,\widehat{\boldsymbol{A}}^{(i-1)} = \boldsymbol{X} - (\boldsymbol{M} - \boldsymbol{I})\,\widehat{\boldsymbol{A}}^{(i-1)}\,, \\ &\quad = \widehat{\boldsymbol{A}}^{(i-1)} + \widetilde{\boldsymbol{F}}^i(\boldsymbol{Y} - \widetilde{\boldsymbol{G}}^i\widehat{\boldsymbol{A}}^{(i-1)})\,. \end{aligned} \quad (3)$$

Many receiver variants can be obtained starting from this expression. A practical receiver would be limited to a few orders, the quality of which depends on the degree of dominance of the useful signal energy carrying static part of the diagonal of $\boldsymbol{M}(n,z)$ given in (3) with respect to its MAI carrying off-diagonal elements and the ICI carrying dynamic contents of the diagonal elements.

In order to increase the dominancy of useful signal carrying part, we revise (3) by replacing MMSE-ZF equalizers with LMMSE equalizers and by introducing ζ symbol feedback nonlinearities which leads us to the multistage receiver architecture in Fig. 3. There, we also demonstrate the option of hard subtracting the pilot tone contribution $\widetilde{\boldsymbol{G}}^P\boldsymbol{A}^P$. After these revisions, the initial formulations should be expanded as:

$$\begin{aligned}\widetilde{\boldsymbol{G}}\,\boldsymbol{A} &= \begin{bmatrix}\widetilde{\boldsymbol{G}}^P & \widetilde{\boldsymbol{G}}^D\end{bmatrix}\begin{bmatrix}\boldsymbol{A}^P \\ \boldsymbol{A}^D\end{bmatrix} \\ \boldsymbol{Y}^D &= \boldsymbol{Y} - \widetilde{\boldsymbol{G}}^P\boldsymbol{A}^P \\ \widehat{\widehat{\boldsymbol{A}}}^{D(-1)} &= 0 \\ \widehat{\boldsymbol{A}}^{D\,(i)} &= \widehat{\widehat{\boldsymbol{A}}}^{D\,(i-1)} + \widetilde{\boldsymbol{F}}^{D\,(i)}(\boldsymbol{Y}^D - \widetilde{\boldsymbol{G}}^{D\,(i)}\widehat{\widehat{\boldsymbol{A}}}^{D\,(i-1)}) \\ \widehat{\widehat{\boldsymbol{A}}}^{D\,(i)} &= \zeta^{D(i)}(\widehat{\boldsymbol{A}}^{D\,(i)})\end{aligned}$$

The superscripts P and D correspond to the pilot-tone and the data parts respectively. In Fig. 3, the numbers in parentheses indicate the iterations where the local functionalities such as equalizers, rechanneling filters and nonlinear symbol estimators reside. These might be optimized according to iteration-dependant residual signal power levels.

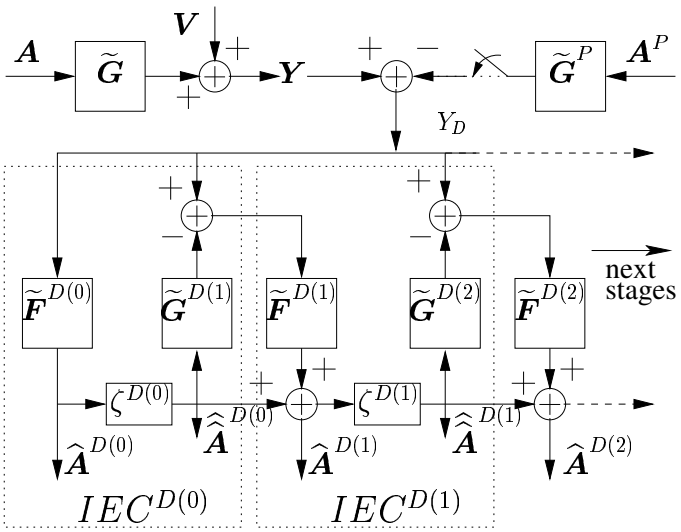

Fig. 3. Polynomial expansion receiver

For the moment, we consider LMMSE chip rate equalizers and exact channel filters within the $\widetilde{\boldsymbol{F}}$ and $\widetilde{\boldsymbol{G}}$ symbol rate filters. In practice, LMMSE equalizer should be implemented as a generalized Rake (G-Rake) receiver [16]. In that case, in every interference estimator and canceller (IEC) block, filtering with $\widetilde{\boldsymbol{F}}$ and $\widetilde{\boldsymbol{G}}$ will have the same complexity of a Rake receiver. Hence, the filtering parts of each iteration will have twice the complexity of those of Rake.

In the straight linear PE case, the ζ symbol estimator is the identity matrix everywhere. Those diagonal parts corresponding to the *known* actual codes, however, can be replaced by symbol feedback functionalities like diagonal weightings, hard-decisions, hyperbolic tangent nonlinearities or even channel decoding and encoding blocks to increase the dominancy of the static contents of the diagonal part of the iteration dependant user cross correlation matrix. To adopt such an hybrid approach, one can utilize properly dimensioned FWHTs or multiple correlators (depending on complexity) as shown in Fig. 2 to move back and forth between the actual symbols of the known codes and their pseudo-symbol equivalents at PE level. The proper way of applying the hyperbolic tangent nonlinearities is to re-estimate the bending parameter (i.e the interference + noise variance) in every iteration. It is simply the difference between the actual symbol power and the moving average estimate of the received symbol powers.

One can apply diagonal weightings also on the symbols of unknown codes. Each linear pseudo-symbol estimate $\widehat{a}_i$, $i \in \{0,\ldots,L-1\}$ have three components: correct pseudo-symbol, interference and colored noise. When we model only one BS and use a linear filter $\boldsymbol{f}$, (LMMSE equalizer, Rake, etc), then $\sigma^2_{\widehat{a}_i} = \sigma^2_{a_i} + (1-\alpha)\,\sigma^2_{TOT}/L + \|\boldsymbol{f}\|^2\sigma^2_v$ where $\{\alpha;\, \sigma^2_{TOT};\, \|\boldsymbol{f}\|^2\}$ represent {orthogonality factor: the ratio

of the magnitude square of the *useful-signal-carrying-tap* of the filter output impulse response to the sum of the magnitude squares of all the taps; sum of the pseudo symbol powers; filter energy}. Grouping the powers of the linearly estimated symbols in a vector, we obtain the following linear system of equations that lead us to the diagonal weights:

$$\widehat{\sigma^2_{\boldsymbol{A}}} = \underbrace{\left(\boldsymbol{I} + \frac{(1-\alpha)}{L}\,\mathbb{1}_L \mathbb{1}_L^T\right)}_{\boldsymbol{P}} \sigma^2_{\boldsymbol{A}} + \underbrace{\|\boldsymbol{f}\|^2 \sigma_v^2\, \mathbb{1}_L}_{\sigma^2_{\boldsymbol{w}}}$$

$$\sigma^2_{\boldsymbol{A}} = \boldsymbol{P}^{-1}\left(\widehat{\sigma^2_{\boldsymbol{A}}} - \sigma^2_{\boldsymbol{w}}\right)$$

$$\zeta = Diagonal\{\frac{\sigma^2_{a_0}}{\widehat{\sigma^2_{a_0}}}, \ldots, \frac{\sigma^2_{a_{(L-1)}}}{\widehat{\sigma^2_{a_{(L-1)}}}}\}$$

$$\hat{\hat{\boldsymbol{A}}} = \zeta\, \hat{\boldsymbol{A}}$$

Another reasonable approach would be to separate the data part into two categories D_1 and D_2 which correspond to multiple HSDSCH codes (i.e codes with known power) and the rest. One might at first instant estimate and cancel the symbols of D_1 via exploiting nonlinearities and then treat the symbols of D_2 linearly by PE. Putting the code of interest in D_1 or D_2 category leads to two different receiver methods which might both be explained on Fig. 4. When we put it in D_2, in an initial step we cancel the interference of HSDSCH codes and then similar to the setting explained in Fig. 3, we iterate on the code of interest with others for a number of PE stages. Hence, there is no need for block 3 in Fig. 4. When we put the code of interest in D_1, however, the initial block cancels the estimated signals of all HSDSCH codes including the signal of interest. In the second block, PE expansion estimates all the remaining interference. Due to the absence of also signal of interest, here we expect a better estimation than the first method. Then, this estimate is deleted from the originally received signal and in the third block interference cancellation is applied among the HSDSCH codes. Although not shown on the figure, it is also possible to iterate many stages in the third block. The second method is clearly more efficient in terms of the implementation cost when there are multicodes of interest. Because, in that case the PE stages would be different for each code of interest when the first approach is adopted.

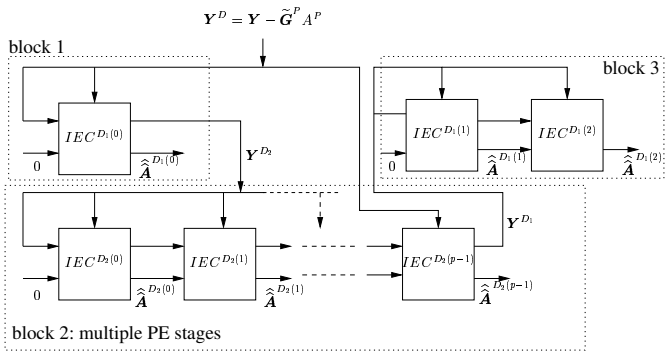

Fig. 4. Hybrid polynomial expansion receiver

Such group partitioned receivers have a serious drawback. If the interference of the known codes is not cancelled very reliably in the first stage, then the leakage interference will result in dramatic deterioration of the performance during following PE stages. To remedy the situation, known codes can be contained in the PE as well. However the improvement w.r.t the straight PE over all known and unknown codes will be very negligible. We believe that such a SIC-PIC-hybrid approach would work well when channel decoding and encoding is adopted as the symbol feedback functionality. This would decrease the leakage below a maximum tolerated value.

IV. SIMULATIONS

For simulations, we consider only the receiver in Fig. 3 with an HSDPA service scenario in the UMTS FDD downlink as follows: There are 5 HSDSCH codes at SF-16 each consuming 8% of the BS power. The pilot tone at SF-256 consumes 10% power. There is the PCCPCH code at SF-256 that consumes 4% power. To effectively model all the rest multirate user codes that we do not know, we place 46 pseudo-codes at level 256 each having 1% power. So in total, 5 HSDSCH codes at SF-16 being equivalent to 80 pseudo-codes at SF-256, the system is effectively 50% loaded. We assume that all the five HSDSCH codes belong to the user of interest; hence they are known. Other than those, we know the code (even the content) of the pilot tone. So we consider hard subtracting it. Although we know the PCCPCH code, we leave it within the group of unknown codes. We model an interfering second BS having the same properties with the only exception that we assume we do not know its HSDSCH codes and hence we treat them only linearly. Although, in practice, the effective codes should be detected by a method explained in the text, for the moment, we assume that they are known. We also assume perfect knowledge of channels. An oversampling factor of $m = 2$ and one receive antenna $q = 1$ are used. The propagation channels are randomly generated from the ITU Vehicular-A channel model. Pulse shape is the UMTS-standard, root-raised cosine with a roll-off factor of 0.22. Therefore the propagation channel, pulse shape cascade (i.e the overall channel) has a length of 19 chips at 3.84 Mchips/sec transmission rate. Symbols are QPSK symbols. Note that for HSDSCHs, 16-QAM is also a possibility but so far we did not consider it.

Fig. 5 shows the SINR versus input Eb/No results. Here we treat all the codes linearly (identity matrix as symbol feedback) and we do not subtract the pilot tone. We consider both LMMSE equalizer and channel matched filter for the chip rate filtering. As seen from the figure, there is a dramatic consequence of choosing one for the other. The performance improves with every iteration when LMMSE equalizers are used whereas the trend is in the reverse direction for the channel matched filters. This result can be attributed to the difference between orthogonality factors at the two filter outputs. One can implicitly see this by observing the 0^{th} iteration outputs d_0 and c_0 where there is more than 6 dB gap between LMMSE-Equalizer and CMF performance. This result indicates that if the initial stage does not perform

good enough, then the iterations will diverge. Provided that divergence is avoided, still the speed of convergence highly depends on the used chip rate filter.

When we look at the performance of equalizers in Fig. 5, we see that the amount of improvement between iterations depend on the input Eb/No (SNR in other words). Early iterations saturate also earlier as we move along increasing Eb/No axis. The difference between two consecutive iterations is negligible until around 10 dB before their very close saturating instants. The size of the cells matter here. In small sized cells, it is possible to have high SNR conditions. This is especially a particular situation in pico and microcells where HSDPA service will be mostly given. In that case, going to a high number of iterations might pay off. In large cells like macro or rural ones, however, noise will become comparable to interference. Then limiting the iterations to 1, or using only the equalizer (i.e iteration 0) or even a Rake replacement would be better since each iteration would then amplify the noise and deteriorate the performance instead of improving it.

We now elaborate on the results in Fig. 6 this time hard subtracting the pilot tones from both BSs and introducing hyperbolic tangent and hard decision functionalities over the HSDSCH codes in the own cell. By first comparing the linear estimates with the linear estimates obtained previously in Fig. 5 we can say that there is very little improvement from pilot tone cancellation. As seen in Fig. 6, we didn't obtain any difference between the performances of hyperbolic tangent and hard decisions either; so we conclude that hard decisions are preferable due to their simplicity. Compared to the linear treatment, however, both perform much better. Furthermore, the gap opens with every iteration. That is to say, for example, the difference at high SNR regions between s_4 or m_4 to c_4 (10 dB) is much higher than the difference between s_1 or m_1 to c_1 (1 dB). High SNR conditions being a more probable deployment scenario, HSDPA will then highly benefit from an high order receiver with proposed nonlinearities.

REFERENCES

[1] S. Tantikovit and A. Sheikh, "Joint multipath diversity combining and mlse equalization (rake-mlse receiver) for wcdma systems," *Proc. Vehicular Technology Conf.*, May 2000.

[2] H. Boujemaa, R. Visoz, and A. Berthet, "A rake-dfse equalizer for the umts downlink," *Proc. Vehicular Technology Conf.*, May 2002.

[3] C. Unger, R. Irmer, and G. Fettweis, "On interpath interference suppression by mlse detection in ds/ss systems," *Proc. Personal, Indoor and Mobile Radio Communications Conf.*, Sept 2003.

[4] D. Divsalar, M. Simon, and D. Raphelli, "Improved parallel interference cancellation," *IEEE Transactions on Communications Theory, Vol.46,pp. 258-268*, Feb 1998.

[5] R. M. Buehrer, S. P. Nicoloso, and S. Gollamudi, "Linear versus nonlinear interference cancellation," *Journal of Communications and Networks, vol.1*, June 1999.

[6] N. Mehta, L. Greenstein, T. Willis, and Z. Kostic, "Analysis and results for the orthogonality factor in wcdma downlinks," *Proc. Vehicular Technology Conference*, May 2002.

[7] K. Pedersen and P. Mogensen, "The downlink orthogonality factors influence on wcdma system performance," *Proc. Vehicular Technology Conference*, September 2002.

[8] "3GPP TS 25.848, Physical Layer Aspects of HSDPA, [Online]. Available:http://www.3gpp.org/ftp/Specs."

[9] "3GPP TS 25.855, UTRA High Speed Downlink Packet Access; Overall UTRAN description, [Online]. Available: http://www.3gpp.org/ftp/Specs."

[10] J. Sadowsky, D. Yellin, S. Moshavi, and Y. Perets, "Cancellation accuracy in cdma pilot interference cancellation," *Proc. Vehicular Technology Conf.*, April 2003.

[11] M. Madcour, S. Gupta, and Y. Wang, "Successive interference cancellation algorithms for downlink w-cdma communications," *IEEE Transactions on Wireless Communications, vol.1, No.1*, Jan 2002.

[12] S. Moshavi, E. Kanterakis, and D. L. Schilling, "Multistage linear receivers for ds-cdma systems," *International Journal of Wireless Information Networks, Vol.3, No.1*, 1996.

[13] R. Irmer, A. Nahler, and G. Fettweis, "On the impact of soft decision functions on the performance of multistage parallel interference cancelers for cdma systems," *Proc. VTC Spring 2001, Rhodes, Greece*, May 2001.

[14] A. Bastug and D. Slock, "Interference cancelling receivers with global mmse-zf structure and local mmse operations," *Proc.Asilomar Conf. on Signals, Systems & Computers*, November 2003.

[15] I. Ghauri and D. T. M. Slock, "Mmse-zf receiver and blind adaptation for multirate cdma," in *Proc. VTC'99*, Sept 1999.

[16] T. O. G. Bottomley and Y. Wang, "A generalized rake receiver for interference suppression," *IEEE Journal Selected Areas Communications*, vol. 18, pp. 1536–1545, August 2000.

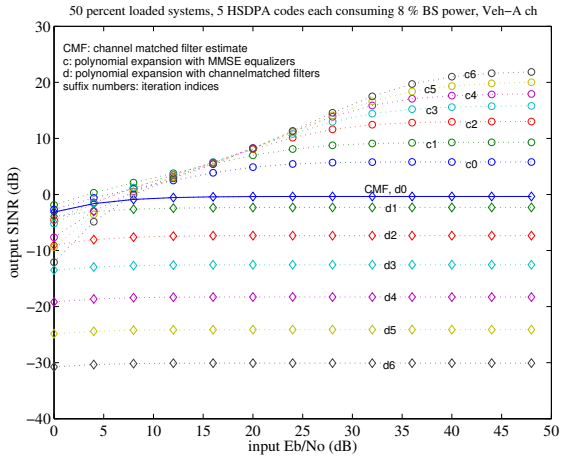

Fig. 5. Polynomial expansion with {channel matched filters, MMSE equalizers}

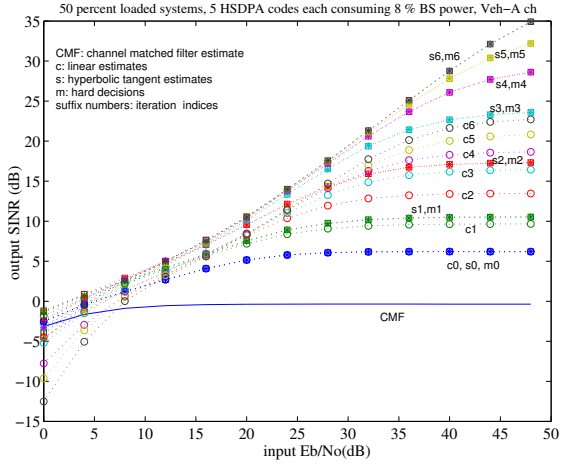

Fig. 6. Polynomial expansion with MMSE equalizers and {linear, hyperbolic tangent, hard} decisions